Three Dimensional Effects in Tokamaks – How Tokamaks Can Benefit From Stellarator Research

S. Günter, M. Garcia-Munoz, K. Lackner, Ph. Lauber, P. Merkel, M. Sempf, E. Strumberger, D. Tekle and the ASDEX Upgrade team

Max-Planck Institut für Plasmaphysik, 85748 Garching, Germany, EURATOM Association

e-mail contact of main author: guenter@ipp.mpg.de

Abstract. The paper deals with three dimensional effects in tokamaks that can be approximated by slowly varying 3d equilibria so that their theoretical description and corresponding code developments can benefit from stellarator research. We investigate the effect of magnetic field ripple and perturbation fields (magnetic islands, external coils) on fast particle orbits in ITER and ASDEX Upgrade equilibria. – The coupling of the plasma perturbation to realistic tokamak wall structures introduces 3d elements into the treatment of Resistive Wall Modes (RWMs). We have developed and successfully benchmarked a RWM code allowing for 3d plasma equilibria and wall geometries. We show that for realistic wall structures the 3d effects remove the degeneracy of +/-n modes and can give rise to significant coupling of modes with different toroidal mode number n. – Kinetic damping of RWMs by plasma rotation is investigated in the low rotation regime relevant for ITER and DEMO. It is found that the inclusion of drift wave physics results in an increased damping for plasma rotation velocities in the range of the diamagnetic frequency due to the resonant excitation of electrostatic plasma waves.

1. Introduction

Although tokamak plasmas are usually considered to be axisymmetric, three dimensional effects are often important. The most obvious is due to the finite number of toroidal field coils and the resulting magnetic field ripple which gives rise to a diffusion of deeply trapped particles. In this paper we discuss in addition several other 3d-effects in tokamaks, emphasizing, in particular situations where synergies have been possible with stellarator research in the development and use of computational tools. We restrict ourselves to situations, where the 3d perturbations grow slowly ($\gamma << v_A/R$), so that the plasma passes through a sequence of ideal-MHD equilibrium states, with the time-dependence determined by the resistive decay of plasma or wall currents (excluding thereby Alfvén-type modes).

Localized current deficits at resonant surfaces in standard-q profile discharges can be induced by conductivity (pellet injection or radiation enhancement) or bootstrap current reduction (NTMs), and can result in ideal-MHD stable helical equilibrium states with closed flux surfaces and evidently good energy and particle confinement. These perturbations lead to losses of fast particles, generally not associated with resonances in velocity space, but similar to those in non-optimized stellarator equilibria. In this context we have investigated the influence of field perturbations like magnetic islands and magnetic field ripple onto the fast particle orbits. On the time scale of the fast ion motion one can consider the 3d equilibrium to be static. We have followed the orbits of NBI ions in ASDEX Upgrade and of α particles in ITER for 3d equilibria including the effects of NTMs, ELM mitigation coils and magnetic ripple perturbations.

Even ideal-MHD unstable low-n modes can be reduced in growth rate by the presence of sufficiently close resistive walls so as to correspond to slowly developing equilibrium states. The consideration of realistic wall structures (with port-holes) in these cases leads, however to a coupling of different toroidal modes, effectively suggesting the use of stellarator codes for their analysis. We have therefore developed a fully 3d linear MHD stability code that deals with realistic structures of the resistive walls (including holes) and have applied it to the planned ITER and a modified ASDEX Upgrade wall geometry. We find that the 3d wall

structures in general break also the degeneracy of +/-n modes in rigorous toroidal symmetry, and give rise to two eigenmodes with close, but distinct growth rates. In addition - in particular for the planned ASDEX Upgrade wall with its large holes - the coupling between modes with various n numbers becomes significant. These 3d effects, but also the possibility that more than one mode can become unstable in a given situation necessitate a feedback system capable of dealing with multiple modes. We have included such a feedback system into our code and have successfully demonstrated feedback stabilization of multiple modes.
Plasma rotation has a strong effect on the predicted mode growth rate, but the magnitude of the rotation and the critical field amplitude for mode locking depend themselves strongly on the damping of rotation by 3d perturbations. In addition, even at a given rotation speed the dispersion relation of the mode depends on kinetic effects. We have therefore utilized the truly (gyro-) kinetic stability code LIGKA - developed originally for fast particle driven instabilities - for the analysis of resistive wall mode damping.

2. Influence of 3d magnetic field perturbations on the orbits of fast ions

Magnetic islands not only influence the confinement properties of the thermal plasma, but also of supra-thermal particles[1,2,3]. The passing particle orbits develop drift islands around surfaces where the unperturbed drift orbits are closed (rational q values for particle motion). For sufficiently large particle velocities, the drift islands deviate from the corresponding islands in the magnetic field structure. For sufficiently large island sizes these drift orbits can become stochastic [4].

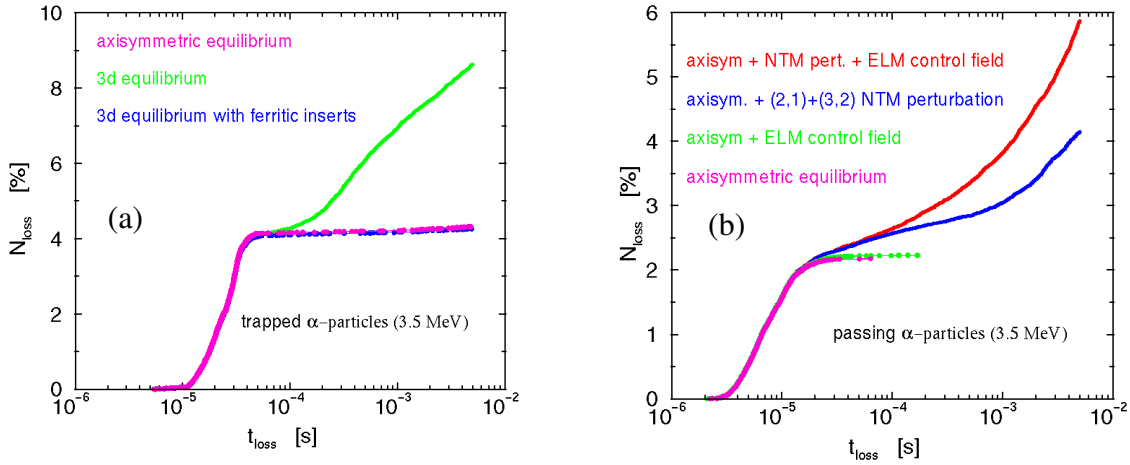

Fig. 1: Losses of α particles in ITER 3d equilibria normalized to the total number of trapped/passing particle orbits followed (a) Trapped particles losses induced by the magnetic field ripple with and without ferritic inserts. (b) Passing particle losses induced by magnetic islands and perturbation fields due to the ELM mitigation coils.

With a new fast ion loss detector recently installed in ASDEX Upgrade, losses of fast ions caused by NTM-produced magnetic islands have been observed, both for well passing and trapped ions. It has been shown [5,6] that well passing ions can get lost on a surprisingly short time scale (order of a few micro seconds), not compatible with diffusive losses. Numerical simulations were able to explain these findings[7], showing that islands in the particle orbits caused by helical field perturbations can come close to or even hit the wall structures. In addition, particle losses on a slower time scale have been observed that could be explained by diffusion due to drift orbit stochastization, caused by both field ripple and magnetic islands.

Ripple losses of energetic particles are also a concern for ITER, but are expected to be strongly reduced by ferritic inserts that partially compensate the ripple. In order to investigate these effects we have followed α particle orbits in 3d ITER equilibria (scenario 2). The starting points of the particles have been chosen to be equidistantly distributed in space and pitch angle. Fig. 1a shows the beneficial effect of the ferritic inserts on α particle orbits in ITER. At least at the nominal magnetic field strength, ripple losses are strongly reduced. In addition to the magnetic field ripple, however, field perturbations caused by magnetic islands and external perturbation fields may result in fast ion losses. These losses have been found to be of particular importance for passing particles (with negative pitch angle) where synergistic effects arise for field perturbations resulting from magnetic islands and from the ELM mitigation coils. Whereas the sole effect of the ELM mitigation coils on the particle orbits is negligibly small, an additional perturbation caused by a (2,1) NTM strongly increases the losses as the particle orbits become stochastic.

3. Three dimensional effects on Resistive Wall Modes (RWMs)

Advanced tokamak scenarios aim at steady state operation with a bootstrap current reaching up to 80 - 90% of the total plasma current. This requires a large normalized plasma pressure (β_{pol}), requiring a careful tailoring of the q-profile to avoid core localized instabilities. The ultimate limit to the normalized plasma pressure is then given by the onset of external kink modes. The growth time of these ideal plasma modes (a few hundred microseconds) can be slowed down significantly (to a few milliseconds) by the presence of conducting walls close to the plasma. The interaction between the plasma and the conducting wall structures, however, introduces additional 3d effects, as the walls will inevitably have holes for heating and diagnostic access. To deal with these effects, we have developed - based on the linear stellarator stability code CAS3D[8] - the STARWALL code[9], which calculates the growth rates of RWMs for walls with arbitrary shape and conductivity in the thin wall approximation. Due to the small growth rate of RWMs, inertia does not play any role for these instabilities and is therefore neglected. The STARWALL code does not need to assume the plasma to be axisymmetric, and it allows - in contrast to other attempts to include realistic 3d wall structures - for the coupling of modes with different toroidal mode numbers *n* introduced by the wall structures and the feedback coil system. The effect of active feedback has been studied using the OPTIM code[10,11], which takes into account all the unstable, and a large set of relevant stable modes found by STARWALL. Like this it treats not only the effect of the feedback system on the unstable modes, but allows also for the changes in the mode structure induced by it and even for the possibility that new modes are driven unstable.

After a successful benchmark of STARWALL, for the case of toroidally closed walls[12], we discuss in the following 3d wall structures. Holes in the walls are of course destabilizing as the magnetic perturbation can penetrate the wall structures more easily (Fig. 2a). The inclusion of the port extensions, however, have a strong stabilizing effect, such that – at least for the n=1 modes considered – the growth rates for the realistic 3d wall structures are only slightly above those for toroidally closed walls (Fig. 2b). Our results agree quite well with those of VALEN[13,14] and CarMa [15,16].

For the ITER scenario 4 equilibrium, the main concern is the n=1 RWM, as modes with toroidal mode numbers larger than 2 are stable up to much higher β_N values (β_N<3.4) which is due to the special shape of the pressure profile. This situation might, however, not be realistic for true steady state scenarios, as for the particular pressure profile the bootstrap current and the total current density are not well aligned. To improve this alignment, the region of large

pressure gradients has to be shifted outwards which might lead to a destabilization of n=2, and even n=3 modes. Such a situation would be much more demanding for a feedback system as it would have to deal with several unstable modes simultaneously. In order to investigate if the latter situation could be handled under realistic conditions, we have generated an equilibrium[17] with more than one unstable mode. Without conducting walls, this equilibrium is linearly unstable against n=1 (β_N >2.2), n=2 (β_N >2.4), and n=3 (β_N >2.4) modes. An ideal wall at a distance of the inner ITER wall would increase these β_N values to 3.65, 2.8, 2.65 for n=1, n=2 and n=3, respectively. Note that the quite large distance between the plasma boundary and the ITER walls does not allow for a significant stabilizing effect onto the n>2 modes and thus limits the achievement of high β_N values for this particular model equilibrium. For walls much closer to the plasma, like envisaged in corresponding DEMO design studies, the achievable β_N values might be significantly larger.

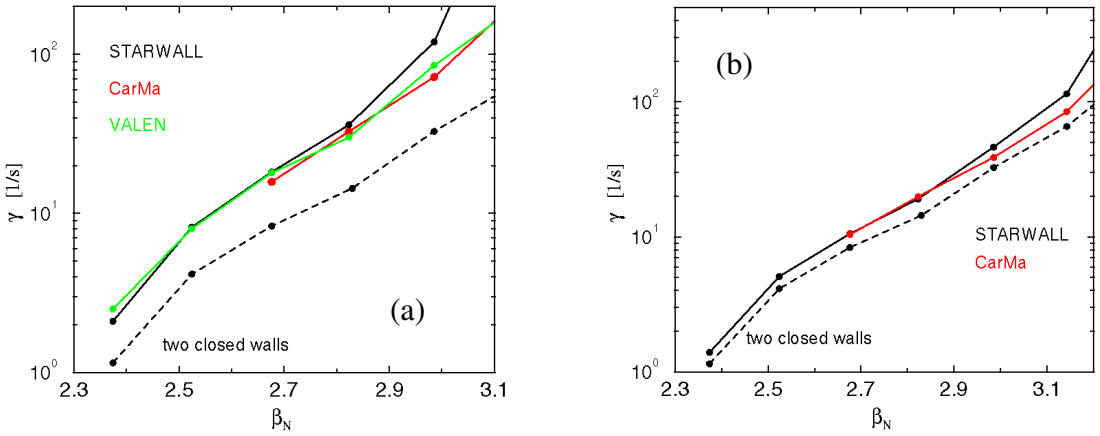

Fig. 2: RWM growth rates vs. β_N for ITER scenario 4 with realistic 3d walls compared to the case of a toroidally closed wall. (a) 3d walls with holes, but without port extensions, (b) with port extensions.

n	ITER 2D	ITER 3D	AUG 2D	**AUG 3D wall, one mode**	**AUG 3D wall n=1,2**
+1	0.72	1.46	1.54	7.12	7.70
-1	0.72	1.46	1.54	6.88	7.50
+2	1.55	4.03	1.67	6.22	6.24
-2	1.55	4.03	1.67	5.84	5.88

Table: Normalised growth rates $\gamma\mu_0\sigma d$ (σ: wall conductivity, d: wall distance) in SI units [1/m] for toroidally symmetric walls (2D) and 3d wall geometry of [17] respectively. For the ASDEX Upgrade wall the coupling between modes with different toroidal mode numbers n becomes important; dominant n: only the dominant +/- n mode included, n=1…2: the four modes considered simultaneously in the analysis.

A corresponding equilibrium has been generated as well for ASDEX Upgrade[17] with the total pressure scaled to achieve similar values of β_N in both machines. For ASDEX Upgrade we use only the additional wall structures that are planned to be inserted for RWM investigations[18], as the distance between the plasma and the present wall is too far to have a significant effect on stability. The table gives the growth rates of the most unstable modes both for an (idealized) toroidally symmetric wall as well as for the realistic 3d structures. In addition

to the destabilizing effect of the holes in the walls, the violation of axisymmetry is able to remove the original degeneracy of +/- n modes, resulting in two modes with different phasing to the wall structures and slightly different growth rates.

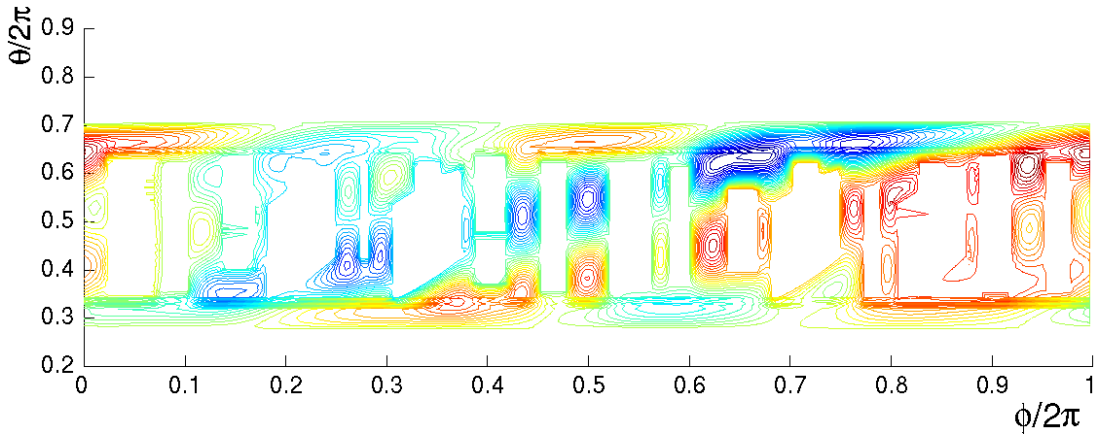

Fig. 3: Contour plot of the current potential Φ ($\vec{j} = \vec{n} \times \nabla\Phi$) *induced by an unstable RWM (normalized growth rate 5.84, see Table) on the wall in ASDEX Upgrade geometry. The vertical and horizontal axes represent the poloidal and toroidal angle, respectively. Note that the mode structure has a pronounced n=1 structure on the outer midplane (θ/2π=0.5), but an obvious n=2 contribution on the upper and lower regions of the wall structures.*

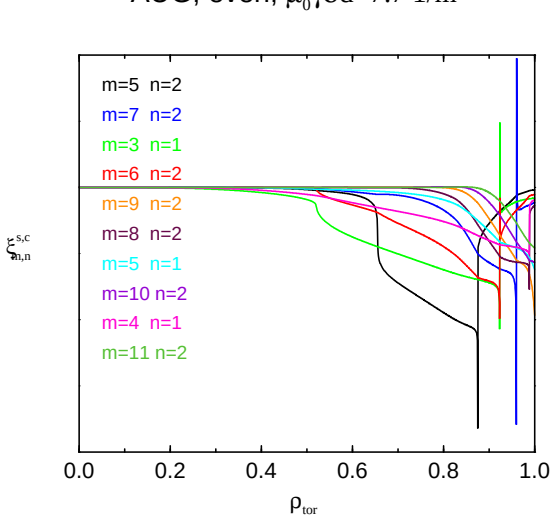

Fig. 4: Fourier harmonics of the radial displacement vs. normalised radius (normalization as in the Table) for the most unstable RWM in ASDEX Upgrade geometry.

This effect is much more pronounced in the case of the ASDEX Upgrade walls where the violation of axisymmetry is much stronger. Within the precision chosen in the Table, the growth rates for +/-n modes in case of the ITER 3D walls agree, whereas one finds a significant difference for the ASDEX Upgrade wall geometry. As discussed above, the coupling to 3d wall structures results also in a coupling of modes with different toroidal mode numbers already in a linear calculation**.** This effect is largest for the n=1 mode in case of the ASDEX Upgrade wall geometry. As shown in the Table the growth rates increase if the coupling to n=2 modes is accounted for. The wall currents and eigenfunctions shown in Figs. 3 and 4 demonstrate the effect of mode coupling as well. The eigenfunction in Fig. 4 exhibits pronounced spikes at the rational surfaces of the respective Fourier harmonics. These spikes are a result of the neglect of plasma inertia in the STARWALL code. Although this approximation is well satisfied considering the very slow growth of the modes, it allows for a strong acceleration of the plasma - otherwise limited by inertia - within the resonant surfaces associated with a finite radial displacement. This effect necessitates a very high spatial

resolution at the rational surfaces, but usually does not significantly influence the growth rates, as demonstrated in the careful benchmarking efforts discussed above.

The simultaneous occurrence of several modes is highly demanding for an effective feedback system. To deal with such a situation we have developed the OPTIM code that uses the results of STARWALL for possible eigenfunctions. In addition to the unstable modes we take into account as well the most important stable modes, as the feedback system might alter the mode structure and thus destabilize originally stable modes. Details on the selection of the most relevant modes as well as of the feedback logic can be found in [10,11]. To demonstrate that feedback on more than one unstable mode is possible, we have applied the OPTIM code to the case of four unstable modes in ASDEX Upgrade, including n=+/-1 and n=+/-2 modes. Using a single toroidal array of 8 equidistantly placed sensors and the feedback coil system discussed in[10] we were able to demonstrate that the feedback coil system as designed is able to stabilize all modes simultaneously. Fig. 5 shows negative values for the growth rates of all modes considered, for some modes the feedback system causes a finite mode frequency.

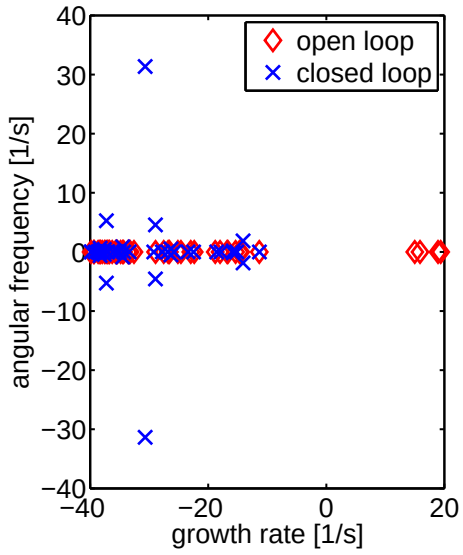

Fig. 5: Growth rate and rotation frequency of RWMs for the ASDEX Upgrade case with n=+/-1 and +/-2 modes included. The four originally unstable modes (open loop) can be stabilized using the feedback coils planned for ASDEX Upgrade (closed loop).

4. Rotation damping of RWMs

As RWMs are unstable only if perturbed magnetic flux is able to penetrate the wall, they cannot grow while rotating with respect to the wall with a frequency significantly larger than the inverse resistive wall time. On the other hand - as the plasma usually rotates much faster - perturbations nearly frozen into the wall frame will be subject to a number of damping mechanisms in the plasma. As the magnetic perturbation and the plasma rotation happen on time scales slow compared to the Alfvén time, the driving MHD part can, in principle, again be considered as a 3d perturbation of the equilibrium. Direct damping of the perturbation in the plasma can then occur by collisional dissipative effects, or by resonances with particle motions. This kind of damping can be well analyzed by a perturbative approach, neglecting its effect onto the structure of the MHD perturbation[19,20]. The motion of the MHD perturbation enforced by its near-freezing to the wall frame can, however, also excite plasma waves through continuum[21,22,23] or discrete resonances, and extract energy in this way.
An instrument suited to study all these effects is the gyrokinetic linear code LIGKA[24]. Although originally developed to study fast particle driven instabilities, it has recently been extended towards low frequency modes[25] so that it can now treat rigorously the coupling of

the shear Alfvén waves to drift and sound waves. As it does, in its present form, not include a vacuum region or plasma rotation we use it in its antenna version[25], imposing the rotating MHD perturbation via boundary conditions (or a virtual antenna), mimicking solutions obtained with the free-boundary CASTOR-FLOW code. Since LIGKA is based on a comprehensive physics model, it can give information on all kind of kinetic damping mechanisms, both acting directly via particle – MHD perturbation resonances, and those corresponding to resonant excitation of secondary waves. The inclusion of diamagnetic drift effects makes it well suited to investigate the low rotation regime of recent experiments with balanced NBI injection[26] which is most important as well for ITER and DEMO.

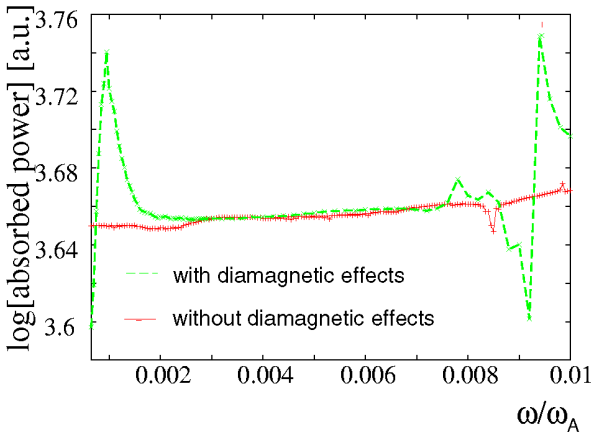

Fig. 6: Absorbed power vs. frequency with and without inclusion of diamagnetic drifts. The inclusion of diamagnetic drifts leads to an increased absorbed power at very low frequencies by about 25% (note the logarithmic scale).

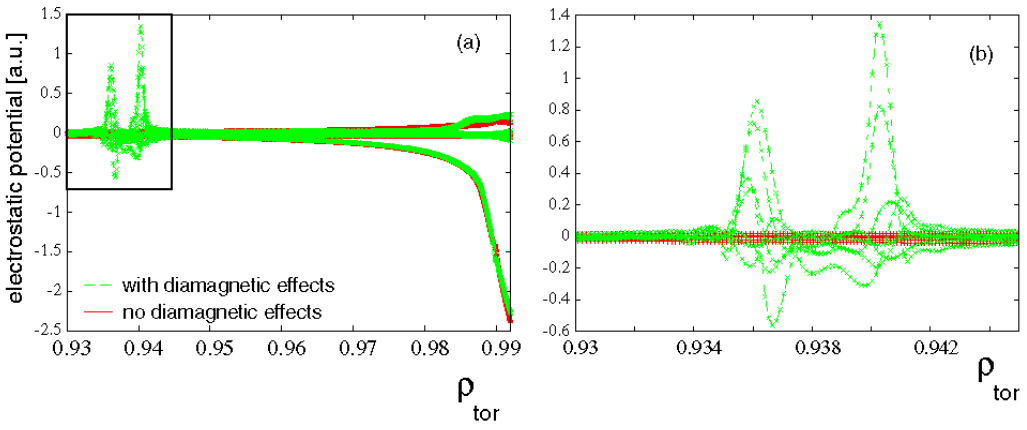

Fig.7: (a) Mode structure (electrostatic potential) at the frequency of maximum absorbed power in Fig.6. (b) Zoom into the region of the excited the electrostatic mode, the green curves correspond to different poloidal mode numbers.

Resonant excitation of secondary modes with n=1 at low frequencies is possible at rational surfaces only where the phase velocity of the modes can equal the plasma rotation frequency. The damping of a wave imposed by the antenna is given by the power absorbed in the plasma, which, for the low frequency range, is shown in Fig. 6. In addition to a number of known resonances at higher frequencies (not shown), we observe, in particular, a broad resonance region around the diamagnetic drift frequency. The mode structure at the frequency of maximum absorbed power is shown in Fig. 7. The inclusion of diamagnetic drifts obviously

allows for the excitation of electrostatic plasma waves with frequencies below ω*, localized at the rational surface. The excitation of these waves significantly increases the absorbed power over quite a broad frequency range. As the spectral width of this range is large compared to the typical inverse resistive wall time, this resonance and the concomitant damping of the MHD perturbation could have a significant influence on the damping of RWMs at low rotation frequencies.

Acknowledgements
The authors would like to thank T. Kurki-Suonio and V. Hynönen for helpful discussions and the supply of the ITER magnetic field data.

References
[1] S. J. Zweben et al., Nucl. Fusion **40**, 91 (2000)
[2] R.B. White and H.E. Mynick, Phys. Fluids **B1**, 980 (1989)
[3] H.E. Mynick, Phys. Fluids **B5**, 1471 (1993)
[4] E.M. Carolipio et al., Nucl. Fusion **42**, 853 (2002)
[5] M. García-Munoz et al., Nucl. Fusion **47**, L10 (2007)
[6] S. Günter et al. Nucl. Fusion **47** 920 (2007)
[7] E. Strumberger et al., NJP **10**, 023017 (2008)
[8] C. Nührenberg, Phys. Plasmas **3**, 2401 (1996)
[9] P. Merkel et al., 21st IAEA Fusion Energy Conference 2006, Chengdu, China (International Atomic Energy Agency, Vienna, 2006), TH/P3-8
[10] M. Sempf, P. Merkel, E. Strumberger, and S. Günter, *Robust control of resistive wall modes in ITER: comparing different feedback coil systems*, 35th EPS Plasma Physics Conference, Heraklion, 2008,
[11] M. Sempf et al., *Robust control of resistive wall modes using pseudospectra*, to be submitted to NJP
[12] S. Günter et al., Plasma Phys. Control. Fusion, in press (October 2008)
[13] J. Bialek, A. Boozer,M.E. Mauel, and A. Navratil, Phys. Plasmas **8**, 2170 (2001)
[14] J. Bialek private communication, 9th ITPA meeting of the MHD TG (2007)
[15] A. Portone et al., Plasma Phys. Control. Fusion **50**, 085004 (2008)
[16] F. Villone et al., RWM control in ITER including a realistic 3D geometry, 35th EPS conference, Hersonissos, 2008, P-2.080
[17] E. Strumberger et al. Phys. Plasmas **15**, 056110 (2008)
[18] W. Suttrop, T. Bertoncelli, V. Bobkov et al., Europhys. Conf. Abstr. **31F**, P-5.119 (2997)
[19] B. Hu and R. Betti, Phys. Rev. Lett. **93**, 105002 (2004)
[20] B. Hu, R. Betti, and J. Manickam, Phys. Plasmas **12**, 057301 (2005)
[21] A. Bondeson and M.S. Chu, Phys. Plasmas **3**, 3013 (1996)
[22] A. Bondeson and D.J. Ward, Phys. Rev. Lett. **72**, 2709 (1994)
[23] L.-J. Zheng, M. Kotschenreuther, and M.S. Chu, Phys. Rev. Lett. **95**, 255003 (2005)
[24] Ph. Lauber et al., J. Comp. Phys. **226**, 447 (2007)
[25] Ph. Lauber, S. Günter, Nucl. Fusion **48**, 084002 (2008)
[26] H. Reimerdes et al., Plasma Phys. Control. Fusion **49**, B349 (2007)